https://doi.org/10.21122/1029-7448-2023-66-3-233-245

UDC 621.316.925

Current Transformer Saturation Detection Method Based on Artificial Neural Network

Yu. V. Rumiantsev[1)]

[1)]Belarusian National Technical University (Minsk, Republic of Belarus)

Abstract. When current transformer is saturated, mainly due to the presence of an exponentially decaying DC component in the fault current, its secondary current has a distinctive distorted waveform which significantly differs from its primary (true) waveform. It leads to an underestimation of the secondary current value calculated by the relay protection compared to its true value. Thus, in its turn, results in trip time delay or even in a relay protection devices operation failure, since its settings and algorithms are calculated and designed on the assumption that the secondary current waveform is sinusoidal and proportional to the primary. And since, when using classical electromagnetic current transformer, it is impossible to exclude the possibility of its saturation, the detection of such abnormal condition is an urgent technical problem. The article proposes to use an artificial neural network for this purpose, which, together with the traditional method of saturation detection based on adjacent secondary current samples comparison, allows implementing a fast and reliable current transformer saturation detector. The article details the stages of the practical implementation of such an artificial neural network. The MATLAB-Simulink environment was used for assess the proposed saturation detector operation. The experiments that had been performed confirmed that proposed method provides fast and accurate saturation detection within the wide range of the power system and current transformer parameters change.

Keywords: current transformer saturation, detection, relay protection, neural network, MATLAB, Simulink

For citation: Rumiantsev Yu. V. (2023) Current Transformer Saturation Detection Method Based on Artificial Neural Network. *Energetika. Proc. CIS Higher Educ. Inst. and Power Eng. Assoc*. 66 (3), 233–245. https://doi.org/10.21122/1029-7448-2023-66-3-233-245

Определение насыщения трансформатора тока на основе использования искусственной нейронной сети

Ю. В. Румянцев[1)]

[1)]Белорусский национальный технический университет (Минск, Республика Беларусь)

Реферат. При насыщении трансформатора тока, преимущественно вследствие наличия экспоненциально затухающей апериодической составляющей в токе повреждения, его вторичный ток имеет характерную непериодическую искаженную форму, существенно отличающуюся от его первичной (истинной) формы, что ведет к занижению вычисляемого релейной защитой значения вторичного тока по сравнению с его истинным значением. Указанное приводит к затягиванию времени срабатывания или вовсе к отказу функционирования устройств

Адрес для переписки
Румянцев Юрий Владимирович
Белорусский национальный технический университет
просп. Независимости, 65/2,
220013, г. Минск, Республика Беларусь
Тел.: +375 17 326-89-51
y.rumiantsev@gmail.com

Address for correspondence
Rumiantsev Yury V.
Belarusian National Technical University
65/2, Nezavisimosty Ave.,
220013, Minsk, Republic of Belarus
Tel.: +375 17 326-89-51
y.rumiantsev@gmail.com

релейной защиты, так как уставки и алгоритмы релейной защиты рассчитаны и построены соответственно из предположения о том, что форма сигнала вторичного тока является синусоидальной и пропорциональной первичному. А поскольку в общем случае при использовании классических электромагнитных трансформаторов тока исключить возможность их насыщения невозможно, то выявление указанного режима функционирования является актуальной технической задачей. В статье предлагается использовать искусственную нейронную сеть, которая совместно с традиционным способом определения насыщения на основе сравнения значений соседних выборок вторичного тока позволяет реализовать быстрый и надежный детектор насыщения трансформатора тока. Детально рассмотрены этапы практической реализации такой искусственной нейронной сети. В среде имитационного моделирования MATLAB-Simulink методом вычислительного эксперимента выполнена проверка функционирования предложенного детектора, которая подтвердила, что он позволяет быстро и безошибочно определять насыщение в широком диапазоне изменения параметров энергосистемы и самого трансформатора тока.

Ключевые слова: насыщение трансформатора тока, определение, релейная защита, нейронная сеть, MATLAB, Simulink

Для цитирования: Румянцев, Ю. В. Определение насыщения трансформатора тока на основе использования искусственной нейронной сети / Ю. В. Румянцев // *Энергетика. Изв. высш. учеб. заведений и энерг. объединений СНГ*. 2023. Т. 66, № 3. С. 233–245. https://doi.org/10.21122/1029-7448-2023-66-3-233-245

Introduction

When current transformer (CT) saturation is detected, the following basic actions can be taken to ensure the correct protection device operation:

1) switching to protection algorithm that ensures the saturated CT secondary current distorted waveform reconstruction [1, 2];

2) blocking of protection device operation [3, 4];

3) switching from standard protection operation algorithm to a specially designed one for operation under CT saturation conditions [5, 6];

4) switching to another settings group, specially calculated for CT saturation conditions.

5) switching to short-window digital filters (sinusoidal-wave based) with aim to operate only on undistorted regions of the secondary current waveform [7, 8].

In microprocessor-based protection devices, all operations are performed on digital samples of monitored continuous analog current and voltage signals. The main parameters of a digital signal are: the sampling rate – the number of samples per fundamental frequency period and the sampling period – time between two adjacent samples [9].

There are a large number of traditional ways to detect instants when CT enters and exits saturation. However, most of the known methods are based on CT secondary current waveform analyzing, which has distinctive features during the beginning and end of the saturation, namely, almost abrupt drop and sharp recovery, respectively.

Using the above noted CT secondary current waveform feature is the simplest and most intuitive method of saturation detection. Because in normal operation condition, the CT secondary current is sinusoidal and similar to the primary one, that's why the difference between adjacent samples cannot exceed a definitely determined value. And taking into account the fact that when CT is saturated, its secondary current waveform is significantly distorted, this difference will significantly exceed this threshold value (which depends on sampling rate and maximum expected fault current level). It should be noted that

the difference between the values of two adjacent samples, in fact, is a first-order finite difference or a similar to it first derivative [10].

One of the earliest references to this CT saturation detection method is given in [11–13]. Later, this method has been further developed, while each author tried to bring some additional features to its implementation.

The greatest development of the considered method was carried out in [14, 15] describing a study that was made of the finite differences of various orders use to detect instants when CT enters and exits saturation. The use of the third finite difference was considered as the most optimal. Also in [14], the influence of a low-pass filter (as part of the protection devices signal conditioning subsystem), which softens the sharpness of the abrupt drop in the secondary current waveform, on the sensitivity of the method is additionally investigated. In [14], it is also has been shown that the correct operation of the proposed method is not affected by the CT core remnant flux presence.

In [16], it is proposed to use the first difference obtained from Lanczos smoothing, which is an effective way to CT saturation detection in case of a secondary current signal with high-frequency noise. In [17], for such a secondary current waveforms, it is proposed to use the second derivative obtained on the basis of the Savitzky – Golay filter. In [18], the finite differences obtained on the basis of Newton's formula are used to their further comparison with the adaptive threshold. In [19, 20], to detect CT saturation, it is proposed to use a special comparison between the secondary current signal, its first and second, second and third finite differences.

All the above mentioned methods for CT saturation detection based in one form or another on the use of the finite differences, have one common drawback: poor performance of detection the instants when CT exits saturation [21, 22]. Also, in most of these methods, a priori knowledge of the maximum expected fault current is required to calculate the threshold.

There are also other ways to CT saturation detection known. In [21], a method based on difference of CT secondary current signal and its second derivative is described. It is known that the sinusoidal signal and its second derivative are in antiphase. Thus, in case of CT saturation absence, the difference between the secondary current signal and its second derivative is approximately zero. Whereas when CT enters and exits saturation, the waveform of such a difference has characteristic peaks, the values of which are compared with predetermined threshold. Also in [21], a method based on difference of averaging and median filters output signals is described.

In [23, 24], a method is described, the essence of which is that the value of the present CT secondary current sample is compared to its predicted value, calculated on the basis of the certain number of previous CT secondary current samples. If this difference is approximately equal to zero, then it is concluded that there is no CT saturation, otherwise it is fixed that CT enters or exits saturation.

Besides the theoretical methods, there are also known methods that have practical implementation in real relay protection devices. Thus, for example, the ABB protection devices use two methods described in technical manuals [25]. The first method is so-called maximum prolongation principle. The essence of this method is to detect the maximum instantaneous CT secondary current value with a help of special algorithm before CT enters saturation and hold this detected value until it exits from it. The operation of the second method is based

on monitoring of the present CT secondary current sample value, finite differences and its comparison with each other and threshold in a specific way [26]. Schneider Electric (Micom) protection devices use a combination of the two following methods for CT saturation detection. The previously considered method for saturation detection based on comparison of the first difference signal with a predetermined threshold, and the second method based on CT core magnetic flux calculation by integrating its secondary current [27]. In Siemens differential protection devices, CT saturation is detected by the fact that in case of the external fault the restraint current rises ahead of the differential current. The delay of the differential current rise is a clear indicator of CT saturation during an external fault [28].

Separately, it should be noted methods based on CT secondary current harmonic composition monitoring. It is known that in case of CT saturation, higher harmonics appears in its secondary current. However, due to the fact that the harmonic content of the secondary current is calculated by digital filters with a window length equal to one fundamental frequency period, the use of such methods for quick detection of CT saturation entry and exit instants is impossible. CT saturation detected by such methods could only be used as an additional factor in complex relay protection algorithms specially designed for operation under CT saturation conditions [29].

There are also other methods of CT saturation detection described: based on CT physical parameters assessment [30], using the wavelet transform [31] and using mathematical morphology [32].

Among the non-traditional methods, the use of artificial neural networks (ANN) can be distinguished [33, 34], which are free from the described above drawbacks. Further, we will consider in more detail the use of ANN for CT saturation detection.

Main part

In [1, 2] artificial neural network architecture and its application to relay protection tasks are considered in detail, the most promising of which are distorted CT secondary current reconstruction and CT saturation detection. Below we will briefly review the implementation steps in the MATLAB-Simulink environment [35] using the Neural Network Toolbox extension package [36] (in the recent versions of MATLAB-Simulink, this package is called Deep Learning Toolbox) in order to use it for the case under consideration.

Figure 1 shows one of the possible ANN topologies. This ANN can be used in MATLAB-Simulink to obtain at its outputs at each sampling step (sampling rate is set to 32 samples per cycle) a signal of presence (SAT) or absence (No SAT) of CT saturation when to ANN's inputs a CT secondary current sliding window is applied. Therefore, the number of inputs and outputs of the ANN should be 32 and 2, respectively.

Once the ANN topology is chosen, it must be trained. Under the training process is understood a set of actions aimed to obtaining on ANN's outputs the desired values for given inputs. For training it is necessary to have a prearranged training dataset, which consist of pairs of input and output values.

For our purpose, training dataset should contain pairs of sampled CT secondary current values (input values) and its associated value of 0 or 1 (output values), indicating the absence or presence of CT saturation, respectively.

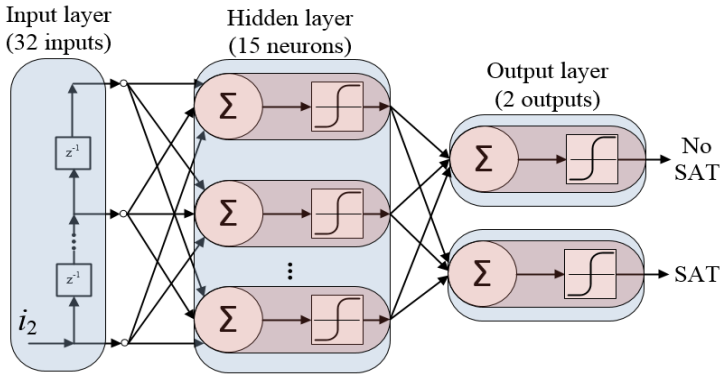

Fig. 1. Artificial neural network topology for current transformer saturation detection

To prepare a training dataset in MATLAB-Simulink using SimPowerSystems extension package [37] (Simscape Power Systems in the latest versions of MATLAB-Simulink), an equivalent power system model was implemented (Fig. 2).

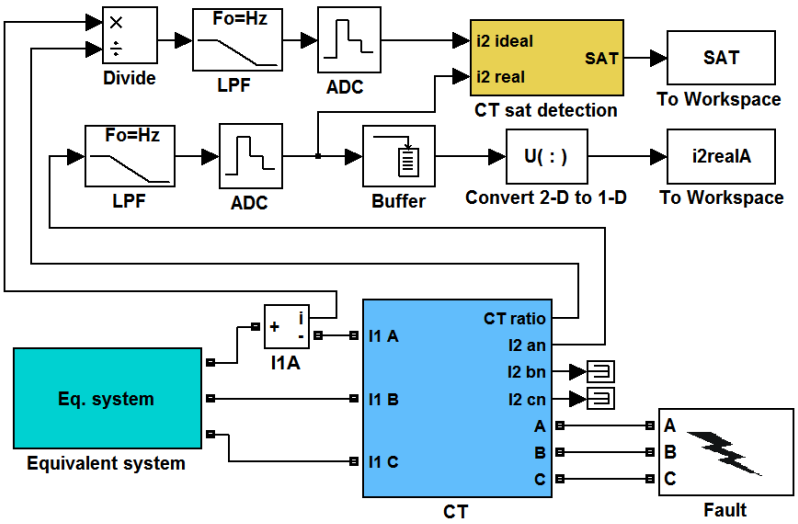

Fig. 2. Training dataset preparation with use of MATLAB-Simulink model of an equivalent power system

The considered model includes the following blocks: equivalent power system (*Equivalent system*), three-phase fault (*Fault*), current transformer (*CT*). It should be noted that due to the lack of a CT model in SimPowerSystems standard library, one was developed and implemented using standard Simulink blocks in accordance with [38]. This *CT* block is able to accurately reproduce both instants when CT enters and exits saturation and the secondary current waveform between these instants.

The rest of the blocks in Fig. 2 are used for analogue filtering, converting analog current signals into digital form and training dataset preparation in such a way that the input (*i2realA*) values of each pair are a digital display of the sliding data window along the CT secondary current. To obtain the output values of each training pair, the sampled CT secondary current values are processed

in a special way by the saturation detection unit (*CT sat detection*), where the values 0 and 1 are formed at its output *SAT*.

The CT model was chosen with the next fixed parameters: CT ratio – 600/5 A (i. e. I_{1n} = 600 A), accuracy limit factor *ALF* – 20, rated secondary burden S_b – 20 VA, actual secondary burden S_a – 20 VA, accuracy class – 10P, no remanent flux B_r i. e. is assumed to be 0 T.

Fault current RMS value I_{sc} changes within the range $0.5I_{1n}ALF$–$3I_{1n}ALF$ A. The time constant τ of the exponentially decaying DC component changes within the range 0–0.1 s. Fault inception angel φ changes within the range 0–360°. Due to the change of φ in the all possible range, the training dataset was prepared using only phase A CT currents.

To prepare a dataset, the step size change of each parameter within the selected range was selected individually, based on the influence of the degree of its change on the resulting distorted CT secondary current waveform. It is done in order to obtain various waveforms of the CT secondary current, and in order to obtain the training dataset adequate size. The process of multiple simulations runs with varying equivalent system parameters of the Simulink model was automated by means of MATLAB code. Considering the above, it was totally obtained the 86016 pairs. The undoubted advantage of MATLAB is that the implemented ANN could be exported to Simulink as a block of its model for further use with other blocks.

The obtained dataset was used for ANN training with the number of neurons in the hidden layer equal to 10, 15 and 20, respectively (Fig. 1).

Hyperbolic tangent sigmoid was applied as a transfer function for hidden and output layers neurons. The scaled conjugate gradient algorithm was used for ANN training. At the same time, to prevent ANN overfitting the early stopping technique was applied. Each ANN was trained 10 times in order to obtain the best performance indexes [39]. The division into training, validation and test datasets was carried out automatically during the ANN training process in the ratio used by default in Neural Network Toolbox – 70 % of the total number of pairs of the dataset is used directly for training, 15 % of the total number of pairs of the dataset is used for validation and test.

It is convenient to evaluate the quality of ANN training process by plotting the training performance index change vs the number of epochs (the number of training algorithm runs). The root mean square error *mse* is often used as a performance index, which reflects the difference between the obtained and expected ANN's output value.

The obtained training results showed that the increasing of the hidden layer neurons from 10 to 15 has a positive effect on the performance index i. e. the *mse* value is significantly reduced. An increase from 15 to 20 neurons did not bring a significant decrease of the *mse*, as a result 20 neurons in hidden layer were deemed inappropriate. Figure 3 shows a log scale plot of the *mse* change on training, validation, and test datasets for ANN with 15 neurons in the hidden layer with the best performance indexes obtained. Training process was stopped at 307 epoch with *mse* = 0.018.

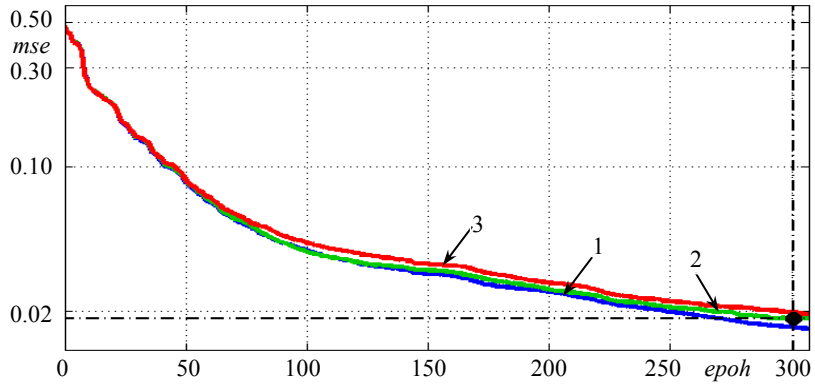

Fig. 3. *Mse* error change during artificial neural network training progress:
1 – training dataset; 2 – validation dataset; 3 – test dataset

One more way to evaluate the training process quality is to use the so-called confusion matrix. On this matrix main diagonal, a number of correctly classified cases are placed and on the off-diagonal elements the misclassified cases are placed. Figure 4 shows the confusion matrix for the obtained ANN, from which it can be seen that 46543 cases of the training dataset are correctly classified as no CT saturation (*No SAT*), 37799 cases are correctly classified as CT saturation (*SAT*). While 643 cases with no saturation are misclassified as CT saturation and 1031 cases with saturation are misclassified as no CT saturation. The total classification accuracy of the obtained ANN is 98 %.

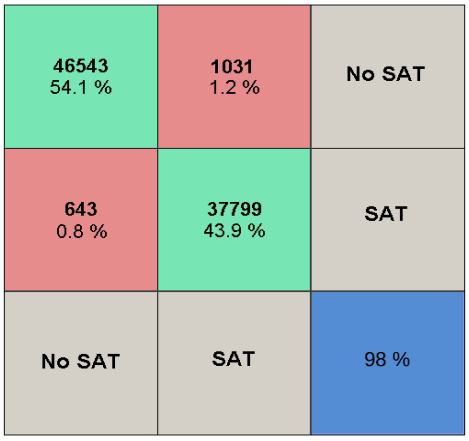

Fig. 4. Confusion matrix of the obtained artificial neural network

It was found during simulations, that, despite of a good performance indexes, in some cases the obtained ANN prone to misclassify CT saturation beginning. And vice versa, a great accuracy of CT saturation ends detection was found.

As it was stated above, CT saturation detection using the third difference Δ^3 method [14] is free from this drawback, but, on the contrary, this method has a poor performance for CT saturation ends detection.

Considering the above, it is proposed to use a combined method for CT saturation detection using the advantages of each method, namely: to detect instants when CT enters saturation use the logical signals from ANN and third difference

method, combined by logical "AND"; to detect instants when CT exits saturation use only logical signal from ANN.

The method of third difference is based on comparison of its value with a predetermined threshold, which depends on the sampling rate and the maximum expected fault current:

$$\left|\Delta^3 = i_{2(n)} - 3i_{2(n-1)} + 3i_{2(n-2)} - i_{2(n-3)}\right| > k\sqrt{2}I_f\left[2\sin\left(\frac{\pi}{N}\right)\right]^3, \quad (1)$$

where Δ^3 is third finite difference; $i_{2(n)}$, $i_{2(n-1)}$, $i_{2(n-2)}$, $i_{2(n-3)}$ are present and previous CT secondary current samples; I_f is maximum expected fault current referred to CT secondary side; N is sampling rate; k is margin factor considering the influence of a low-pass filter.

And if the sampling rate is often known in advance (in our case $N = 32$), then the following difficulties are arise with the use of maximum expected fault current I_f. Firstly, I_f value should be preliminary calculated, which is not always possible because of lack of the source data. Secondly, due to the often power system topology change, the I_f value requires its frequent recalculations. Thirdly, the use of I_f coarsens the threshold (i. e. obtained in accordance with (1) threshold appears higher than it should be), since the actual fault current will almost always have a smaller then I_f value.

The use instead of I_f the actual fault current value calculated in real time by the protection device digital filter, for example, cosine digital filter or digital filter based on the discrete Fourier transform (DFT) [40] makes it possible to cope with all these difficulties. The proposed solution is only applicable for faults, which do not lead to CT saturation, since only when the primary fault current is completely transformed into secondary circuits; these digital filters are able to calculate the true actual fault current value.

In case of faults accompanied by CT saturation, due to incomplete fault current transformation into secondary circuits, the use of traditional digital filters leads to the underestimation of the calculated actual fault current compared to its true actual value.

To obtain the true actual fault current value it is proposed to use a patented digital current measurement element (CME) for operation during current transformer saturation [5, 41, 42]. This CME produces at its output an equivalent current signal which is as close as possible to the true actual fault current value. At the same time, when CT saturation is not observed, this CME operates as a standard digital filter. Figure 5 shows the implementation in MATLAB-Simulink environment of the saturation detector based on proposed combined method.

In addition to the previously observed blocks, Fig. 5 shows the current measurement element *CME* block, the *3rd difference* block for CT saturation detection based on third difference method in accordance with (1), and the *ANN* block of the obtained neural network. At the *No SAT* and *SAT* outputs of *ANN* block corresponding signals are appear.

Consider the operation of the proposed combined method on the example of its use for CT saturation detection. It should be noted that during the training dataset preparation, the CT secondary parameters remained unchanged, and only the equivalent power system parameters has been changed.

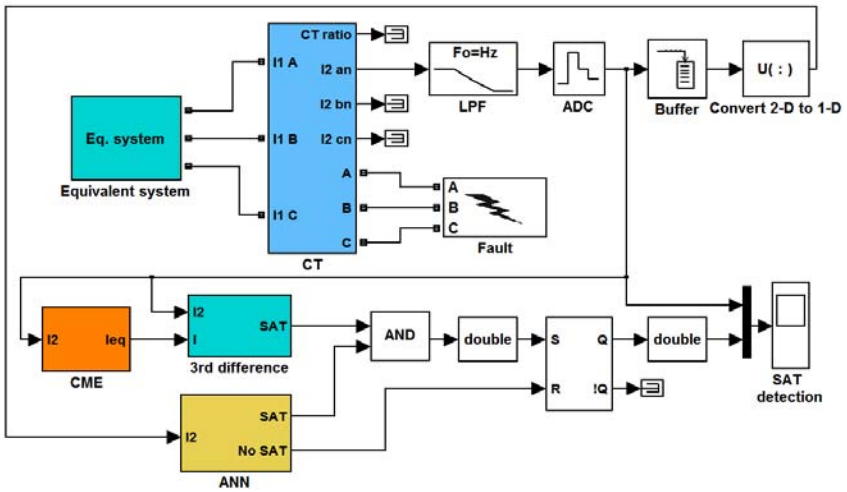

Fig. 5. MATLAB-Simulink based model for current transformer saturation detection with a use of proposed combined method

And vice versa, during computational experiments, CT secondary parameters have been changed within the next ranges: ALF = (10–30), S_a = (10–30) VA, B_r = (–0.8–0.8) T. Additionally, CT saturation curve modeling method is also has been changed, viz. piecewise linear approximation or approximation using the empirical Ollendorf's equation [38]. It was done in order to evaluate the proposed combined method operation in a wide range of power system and CT parameters change.

A large number of computational experiments were performed with various combinations of both the power system parameters and the parameters of CT model. The typical operation results of the proposed combined method are depicted in Fig. 6–8.

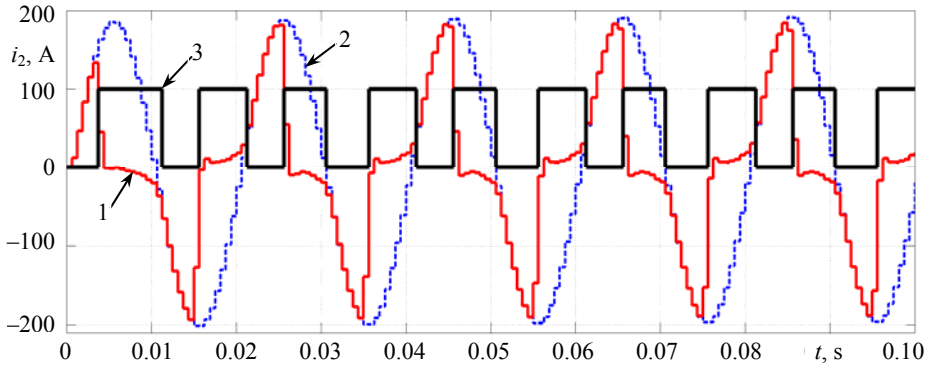

Fig. 6. Saturation detector operation results at I_{sc} = 16547 A, φ = 90°, τ = 0.065 s: 1 – real current transformer secondary current; 2 – ideal current transformer secondary current; 3 – saturation detector output signal

Figure 6 shows an example of AC saturation of CT. The signal from the saturation detector based on proposed combined method is scaled and plotted on each figure below in order to evaluate its operation. An abrupt change in its

signal from 0 to 100 means that CT enters saturation and, conversely, a signal change from 100 to 0 means that CT exits saturation.

For each considered example, CT secondary parameters have been chosen in such a way that they did not match the CT parameters during training dataset preparation. Additionally, for each case, the positive or negative remanent flux was taken into account. Next, we will consider an example of DC saturation with differrent fault inception angles (Fig. 7, 8).

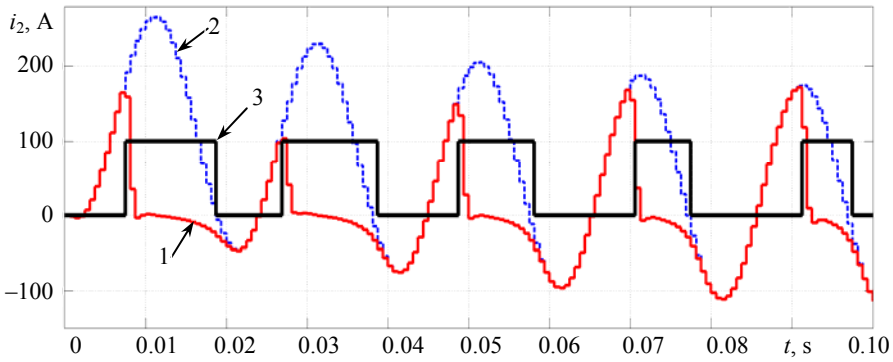

Fig. 7. Saturation detector operation results at I_{sc} = 12456 A, φ = 346°, τ = 0.057 s:
1 – real current transformer secondary current; 2 – ideal current transformer secondary current;
3 – saturation detector output signal

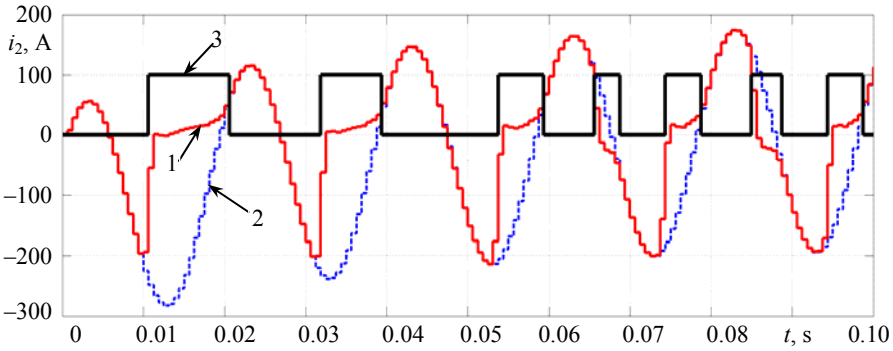

Fig. 8. Saturation detector operation results at I_{sc} = 15850 A, φ = 133°, τ = 0.033 s:
1 – real current transformer secondary current; 2 – ideal current transformer secondary current;
3 – saturation detector output signal

The obtained during numerous computational experiments results are confirmed the exceptional accuracy of the proposed CT saturation detection method based on ANN and third finite difference. It provides quickly and accurately detection of instants when CT enters and exits saturation, regardless of the saturation type, presence of remanent flux, degree of CT saturation and its secondary parameters.

The minor delay in detection of such instants is appeared because of the fact that for reliable detector operation, it is necessary that the condition for its pickup (drop out) be satisfied for a time equal to two consecutive samples of the CT secondary current.

The proposed saturation detection combined method can also be used not only for CT_1 with the help of which training dataset was obtained, but also for

CT_2 with a different from CT_1 ratio. The main condition is that the I_{sc} value must belong to the next range $0.5I_{1n}$ *ALF*–$3I_{1n}$ *ALF* A, where the value of I_{1n} refers to CT_2 and the ALF refers to CT_1.

Consider the detector operation for CT with I_{1n} = 1000 A (Fig. 9). In this example, CT parameters were specially chosen in such a way as to obtain a complex secondary current waveform, due to CT deep saturation. As can be seen from the presented figure, the saturation detector accurately recognizes all the specific instants of complex secondary current waveform, obtained with CT secondary parameters far beyond the range used for dataset preparing.

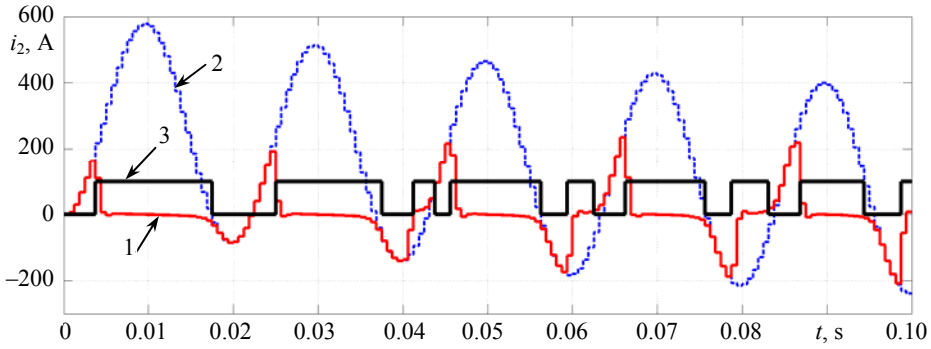

Fig. 9. Saturation detector operation results at I_{sc} = 44543 A, φ = 16°, τ = 0.072 s:
1 – real current transformer secondary current; 2 – ideal current transformer secondary current;
3 – saturation detector output signal

It can be concluded, that the proposed combined method based on ANN and third finite difference can be successfully implemented in real protection devices for quickly and accurately CT saturation detection in order to ensure its correct operation under this abnormal condition. This can be achieved by relay protection blocking or by switching from standard protection operation algorithm to a specially designed for operation under CT saturation conditions.

A distinctive feature of the proposed combined method is the lack of necessity in preliminary threshold calculation, because the required value of the fault current is estimated in real time by a patented digital current measurement element.

CONCLUSIONS

1. The successful possibility of artificial neural networks using for current transformer saturation detection is shown.
2. The proposed combined method provides fast and accurate saturation detection within the wide range of power system and current transformer secondary parameters change.
3. The application of the proposed combined method does not require a preliminary threshold calculation.
4. The implementation of the proposed combined method in real protection devices will ensure their correct operation under current transformers saturation conditions.

REFERENCES

1. Rumiantsev Yu. V., Romaniuk F. A. (2021) An Artificial Neural Network Developed in MATLAB-Simulink for Reconstruction a Distorted Secondary Current Waveform. Part 1. *Energetika. Izvestiya Vysshikh Uchebnykh Zavedenii i Energeticheskikh Ob'edinenii SNG* =

Energetika. Proceedings of CIS Higher Education Institutions and Power Engineering Associations, 64 (6), 479–491. https://doi.org/10.21122/1029-7448-2021-64-6-479-491 (in Russian).
2. Rumiantsev Yu. V., Romaniuk F. A. (2022) An Artificial Neural Network Developed in MATLAB-Simulink for Reconstruction a Distorted Secondary Current Waveform. Part 2. *Energetika. Izvestiya Vysshikh Uchebnykh Zavedenii i Energeticheskikh Ob'edinenii SNG = Energetika. Proceedings of CIS Higher Education Institutions and Power Engineering Associations,* 65 (1), 5–21. https://doi.org/10.21122/1029-7448-2022-65-1-5-21 (in Russian).
3. Rebizant W., Hayder T., Schiel L. (2004) Prediction of CT Saturation Period for Differential Relay Adaptation Purposes. *International Conference on Advanced Power System Automation and Protection,* 1–6.
4. Rumiantsev Yu. V. (2016) A Comprehensive Model for the Power Transformer Digital Differential Protection Functioning Research. *Energetika. Izvestiya Vysshikh Uchebnykh Zavedenii i Energeticheskikh Ob'edinenii SNG = Energetika. Proceedings of CIS Higher Education Institutions and Power Engineering Associations,* 59 (3), 203–224. https://doi.org/10.21122/1029-7448-2016-59-3-203-224 (in Russian).
5. Rumiantsev Yu. V., Romaniuk F. A., Rumiantsev V. Yu., Novash I. V. (2018). Digital Current Measurement Element for Operation during Current Transformer Severe Saturation. *Energetika. Izvestiya Vysshikh Uchebnykh Zavedenii i Energeticheskikh Ob'edinenii SNG = Energetika. Proceedings of CIS Higher Education Institutions and Power Engineering Associations,* 61 (6), 483–493. https://doi.org/10.21122/1029-7448-2018-61-6-483-493 (in Russian).
6. Zocholl S. E., Mooney J. (2004) Primary High-Current Testing of Relays with Low Ratio Current Transformers. *57th Annual Conference for Protective Relay Engineers,* College Station, TX, USA, 182–189. https://doi.org/10.1109/CPRE.2004.238491.
7. Bhide S. R. (2014) *Digital Power System Protection*. PHI Learning Pvt. Ltd. 280.
8. Schneerson E. M. (2007) *Digital Relay Protection*. Moscow, Energoatomizdat Publ. 549 (in Russian).
9. Romaniuk F., Rumiantsev V., Novash I., Rumiantsev Y., Boiko O. (2016) Comparative Assessment of Digital Filters for Microprocessor-Based Relay Protection. *Przegląd Electrotechniczny,* 1 (7), 130–133. https://doi.org/10.15199/48.2016.07.28.
10. Hamming R. (2012) *Numerical Methods for Scientists and Engineers*. 2nd ed. New York, Dover Publications. 721.
11. Evans F. J., Wells G. (1970) Use of a Sampling Scheme to Detect Transient Saturation in Protective Current Transformers. *IEEE Transactions on Instrumentation and Measurement,* 19 (3), 144–147. https://doi.org/10.1109/TIM.1970.4313884.
12. Yang L., Dolloff P. A., Phadke A. G. (1990) A Microprocessor Based Bus Relay Using a Current Transformer Saturation Detector. *Proceedings of the Twenty-Second Annual North American Power Symposium.* Auburn, AL, USA, 193–202. https://doi.org/10.1109/NAPS.1990.151372.
13. Phadke A. G., Thorp J. S. (2009) *Computer Relaying for Power Systems.* 2nd ed. Hertfordshire–Chichester, Research Studies Press Limited and John Wiley & Sons. 344. https://doi.org/10.1002/9780470749722.
14. Kang Y. C., Ok S. H., Kang S. H. (2004) A CT Saturation Detection Algorithm. *IEEE Transactions on Power Delivery,* 19 (1), 78–85. https://doi.org/10.1109/TPWRD.2003.820200.
15. Kang Y. C., Ok S. H., Kang S. H. (2001) A Novel CT Saturation Detecting Algorithm Unaffected by a Remanent Flux. *2001 Power Engineering Society Summer Meeting. Conference Proceedings,* (Cat. No.01CH37262), 1324–1327. https://doi.org/10.1109/PESS.2001.970268.
16. Schettino B. M., Duque C. A., Silveira P. M., Ribeiro P. F., Cerqueira A. S. (2014) A New Method of Current-Transformer Saturation Detection in the Presence of Noise. *IEEE Transactions on Power Delivery,* 29 (4), 1760–1767. https://doi.org/10.1109/TPWRD.2013.2294079.
17. Schettino B. M., Duque C. A., Silveira P. M. (2016) Current-Transformer Saturation Detection Using Savitzky – Golay Filter. *IEEE Transactions on Power Delivery*, 31 (3), 1400–1401. https://doi.org/10.1109/tpwrd.2016.2521327.
18. Chothani N. G., Bhalja B. R. (2014) New Algorithm for Current Transformer Saturation Detection and Compensation Based on Derivatives of Secondary Currents and Newton's Backward Difference Formulae. *IET Generation, Transmission & Distribution*, 8 (5), 841–850. https://doi.org/10.1049/iet-gtd.2013.0324.
19. Dos Santos E. M., Cardoso G., Farias P. E., De Morais A. P. (2012) CT Saturation Detection Based on the Distance between Consecutive Points in the Plans Formed by the Secondary Current Samples and their Difference-Functions. *IEEE Transactions on Power Delivery*, 28 (1), 29–37. https://doi.org/10.1109/TPWRD.2012.2220382.
20. Kumar K., Kumbhar G. B., Mahajan S. (2016) A New Efficient Algorithm to Detect Current Transformer Saturation. *2016 IEEE Power and Energy Society General Meeting (PESGM).* Boston, MA, 1–5. https://doi.org/10.1109/PESGM.2016.7741583.

21. Kasztenny B., Rosolowski E., Lukowicz M., Izykowski J. (1997) Current Related Relaying Algorithms Immune to Saturation of Current Transformers. *Sixth International Conference on Developments in Power System Protection.* Nottingham, Publication No 434, 365–368. https://doi.org/10.1049/cp:19970100.
22. Biswal S., Biswal M. (2019) Detection of Current Transformer Saturation Phenomenon for Secured Operation of Smart Power Network. *Electric Power Systems Research*, 175, 105926. https://doi.org/10.1016/j.epsr.2019.105926.
23. Wiszniewski A., Rebizant W., Schiel L. (2008) Correction of Current Transformer Transient Performance. *IEEE Transactions on Power Delivery*, 23 (2), 624–632. https://doi.org/10.1109/tpwrd.2008.915832.
24. Allain R., Jean P. (2003) *Method for Detecting Saturation in a Current Transformer*. Patent No US10/502,855.
25. *Distributed Busbar Protection REB500. Application Manual*. Available at: https://library.e.abb.com/public/e351d17bb0bf42938f2323a4395b5eea/1MRK505333-UEN_-_en_Application_Manual__REB500_8.10__IEC.pdf.
26. Saha M. (1992) *Method and Device for Detecting Saturation in Current Transformers*. Patent No EP0506035B1.
27. *Easergy MiCOM P740 Differential Busbar Protection Relay, SW Version B1, Manual (Global File) P740/EN M/Qd9*. Available at: https://www.se.com/ww/en/download/document/P74x_EN_M_Qd9__B1_LM.
28. Ziegler G. (2012) *Numerical Differential Protection: Principles and Applications*. 2nd ed. Erlangen, John Wiley & Sons. 287.
29. Benmouyal G., Zocholl S. E., Guzman-Casillas A. (2004) *Instantaneous Overcurrent Element for Heavily Saturated Current in a Power System*. Patent No US6757146 B2.
30. Rebizant W., Wiszniewski A., Schiel L. (2008) CT Saturation Correction Based on the Estimated CT Saturation Time Constant. *2008 IET 9th International Conference on Developments in Power System Protection (DPSP 2008),* 174–179. https://doi.org/10.1049/cp:20080031.
31. Ribeiro P. F., Duque C. A., Ribeiro P. M., Cerqueira A. S. (2013) *Power Systems Signal Processing for Smart Grids*. Chichester, John Wiley & Sons. 448. https://doi.org/10.1002/9781118639283.
32. Wu Q. H., Lu Z., Ji T. (2009) *Protective Relaying of Power Systems Using Mathematical Morphology*. London – New York, Springer Science & Business Media. 207. https://doi.org/10.1007/978-1-84882-499-7.
33. Rebizant W., Szafran J., Wiszniewski A. (2011) *Digital Signal Processing in Power System Protection and Control*. London, Springer Publ. 316. https://doi.org/10.1007/978-0-85729-802-7.
34. Ali M., Son D. H., Kang S. H., Nam S. R. (2017) An Accurate CT Saturation Classification Using a Deep Learning Approach Based on Unsupervised Feature Extraction and Supervised Fine-Tuning Strategy. *Energies*, 10 (11), 1830. https://doi.org/10.3390/en10111830.
35. Dabney J. B., Harman T. L. (2004). *Mastering Simulink*. Upper Saddle River: Pearson/Prentice Hall. 376.
36. *Neural Network Toolbox. User's Guide. Version 4*. The MathWorks, 2002. Available at: http://cda.psych.uiuc.edu/matlab_pdf/nnet.pdf.
37. *SimPowerSystems. User's Guide. Version 5*. The MathWorks, 2011. Available at: https://guides simo.com/document/558673/matlab-simpowersystems-5-operation-user-s-manual-403.html.
38. Novash I. V., Rumiantsev Yu. V. (2015) A Simplified Model of Three-Phase Bank of Current Transformers in the Dynamic Simulation System. *Energetika. Izvestiya Vysshikh Uchebnykh Zavedenii i Energeticheskikh Ob'edinenii SNG = Energetika. Proceedings of CIS Higher Education Institutions and Power Engineering Associations,* (5), 23–38 (in Russian).
39. Hagan M. T., Demuth H. B., Beale M. H., De Jesus O. (2014) *Neural Network Design*. 2nd ed. Boston, PWS Publishing. 1012.
40. Rumiantsev Yu. V., Romaniuk F. A., Rumiantsev V. Yu., Novash I. V. (2016) Digital Filters Implementation in Microprocessor-Based Relay Protection. *Energetika. Izvestiya Vysshikh Uchebnykh Zavedenii i Energeticheskikh Ob'edinenii SNG = Energetika. Proceedings of CIS Higher Education Institutions and Power Engineering Associations,* 59 (5), 397–417. https://doi.org/10.21122/1029-7448-2016-59-5-397-417 (in Russian).
41. Rumiantsev Yu. V., Romaniuk F. A., Rumiantsev V. Yu., Novash I. V. (2017) *Current Measurement Element for Operation during Current Transformer Magnetic Core Severe Saturation*. Patent BY No 20808 C1 (in Russian).
42. Novash I. V., Romaniuk F. A., Rumiantsev V. Yu., Rumiantsev Yu. V. (2021) *Microprocessor-Based Overcurrent Relay Protection Devices: Theory, Modeling, Practices.* Minsk, Belarusian National Technical University. 168 (in Russian).

Received: 2 February 2023 Accepted: 4 April 2023 Published online: 31 May 2023